

# High-pressure behavior of $\text{As}_2\text{O}_3$ : Amorphous-amorphous and crystalline-amorphous transitions

E. Soignard,<sup>1,2,\*</sup> S. A. Amin,<sup>1</sup> Q. Mei,<sup>1,3</sup> C. J. Benmore,<sup>3</sup> and J. L. Yarger<sup>1,\*</sup>

<sup>1</sup>*Department of Chemistry and Biochemistry, Arizona State University, Tempe, Arizona 85287-1604, USA*

<sup>2</sup>*LE-CSSS, Arizona State University, Tempe, Arizona 85287-1704, USA*

<sup>3</sup>*Intense Pulsed Neutron Source and X-ray Science Divisions, Argonne National Laboratory, Argonne, Illinois 60439, USA*

(Received 14 September 2007; revised manuscript received 31 March 2008; published 24 April 2008)

The room temperature compression of  $\text{As}_2\text{O}_3$  has been studied by *in situ* diamond anvil cell Raman and x-ray diffraction up to a pressure of 35 GPa. Upon compression, we discovered a crystal-to-amorphous transition in arsenolite, while claudetite, which is another crystalline polymorph of  $\text{As}_2\text{O}_3$ , remains crystalline up to at least 40 GPa. We have also observed an amorphous-amorphous transition in  $\text{As}_2\text{O}_3$  glass at 25 GPa. This transition is characterized by a dramatic change in the Raman spectrum, which is reversible upon decompression. *In situ* diamond anvil cell x-ray diffraction of  $\text{As}_2\text{O}_3$  glass reveals that the amorphous-amorphous transition is associated with an increase in the arsenic coordination. The amorphous-amorphous transition is reversible with little hysteresis.

DOI: [10.1103/PhysRevB.77.144113](https://doi.org/10.1103/PhysRevB.77.144113)

PACS number(s): 61.43.Fs, 61.05.C-, 78.30.-j, 81.40.Vw

## I. INTRODUCTION

There are three known crystalline  $\text{As}_2\text{O}_3$  polymorphs, arsenolite, claudetite I, and claudetite II.<sup>1-3</sup> All three polymorphs are built from an assembly of  $\text{AsO}_3$  pyramids. In each structure, the As-O bond distance is close to 1.8 Å and the closest As-As distance is approximately 3.2 Å. Arsenolite is the low temperature polymorph [stable below 110 °C (Ref. 4)] that crystallizes into a cubic lattice. In the arsenolite structure, the  $\text{AsO}_3$  building blocks are assembled together to form adamantane structured  $\text{As}_4\text{O}_6$  molecular units (Fig. 1).<sup>1</sup> Claudetite I and II are formed at high temperature and crystallize into a monoclinic lattice. In both forms, each oxygen atom is shared between two  $\text{AsO}_3$  pyramids to form a layered structure.<sup>2,3</sup>

Since 1939,  $\text{As}_2\text{O}_3$  is known to be a good glass forming substance.<sup>5</sup> The local structure of the glass is well known and based on  $\text{AsO}_3$  pyramids. However, the linkage of these building blocks is not as well understood. Imaoka and Hasegawa<sup>6</sup> concluded that a structure consisting of three-membered rings of  $\text{AsO}_3$  pyramids was most consistent with their x-ray diffraction data. Similarly, Clare *et al.*<sup>7</sup> found their neutron data to be consistent with a random network of corner sharing  $\text{AsO}_3$  pyramids with the presence of three-membered rings similar to those found in  $\text{As}_4\text{O}_6$  molecules. These authors also specified that the interplanar distances of either claudetite form are inconsistent with the data. Papatheodorou and Solin,<sup>8</sup> by using Raman spectroscopy, interpreted the structure of  $\text{As}_2\text{O}_3$  glass (*g*- $\text{As}_2\text{O}_3$ ) at high temperature to be layerlike, similar to claudetite. Based on their Raman and infrared data, Galeener *et al.*<sup>9</sup> concluded that the structure of *g*- $\text{As}_2\text{O}_3$  is a continuous random network of  $\text{AsO}_3$  pyramidal units, which is in some way similar to that of  $\text{GeO}_2$  glass. The more recent study by Yannopoulos *et al.*<sup>10</sup> indicated that  $\text{As}_2\text{O}_3$  is a strong liquid ( $m \approx 19$ ) similar to  $\text{SiO}_2$ .<sup>11</sup> These data would indicate that the structure of liquid  $\text{As}_2\text{O}_3$  is a continuous three-dimensional network and not a layered structure or a molecular liquid.

To date, there have been few reports of  $\text{As}_2\text{O}_3$  at high pressure. In 1967, White *et al.*<sup>4</sup> reported the high-pressure

phase diagram of  $\text{As}_2\text{O}_3$  up to 10 GPa. In 1999, Grzechnik<sup>12</sup> reported the compressibility and vibrational modes for arsenolite up to 16 GPa. In that study, the author did not observe

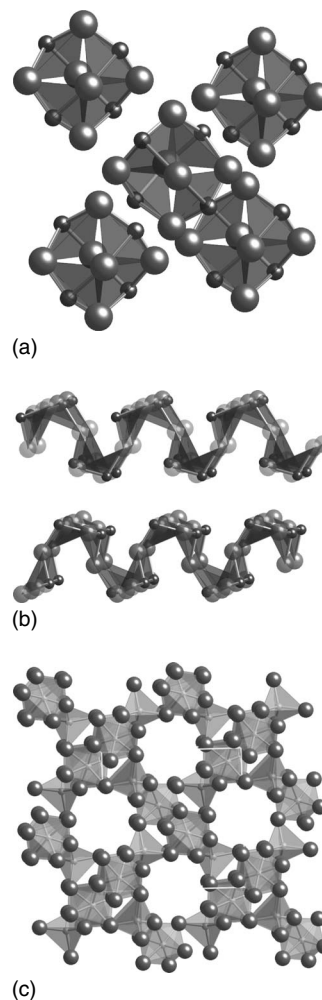


FIG. 1. Structure of (a) arsenolite (*c*- $\text{As}_2\text{O}_3$ ), (b) claudetite I (*m*- $\text{As}_2\text{O}_3$ ), and (c)  $\text{As}_2\text{O}_5$ . In each figure, the large spheres represent the O atoms and the small spheres represent the As atoms.

any structural change in arsenolite. In 2006, Andrikopoulos *et al.*<sup>13</sup> reported the pressure dependence of  $\text{As}_2\text{O}_3$  glass Raman spectrum up to 9.4 GPa. In that study, the authors reported a broadening and a decrease in the intensity of the Raman bands. They interpreted the changes in the local order to be from cagelike structures to layerlike ones. They also concluded that the high-pressure structural modification is retained after pressure release. Finally, in 2007, Mei *et al.*<sup>14</sup> studied the structural changes in pressure densified glassy  $\text{As}_2\text{O}_3$  as well as the pressure dependence of the Raman spectrum up to 11.6 GPa. They concluded that the only structural difference between the samples recovered from 10 and 23 GPa and the starting glass is a small decrease in the As-As-As/O angle, which indicates a slightly tighter packing of  $\text{AsO}_3$  pyramids with increasing density. Below, we extend the range of pressure to 40 GPa and show that significant structural changes in  $\text{As}_2\text{O}_3$  happen in the 20–40 GPa region.

## II. EXPERIMENTAL METHODS

We synthesized both crystalline and glassy  $\text{As}_2\text{O}_3$  from a starting material of 99.99%  $\text{As}_2\text{O}_3$ , which is purchased from Alfa Aesar (Lot No. 032681). The samples produced were thermally quenched *g*- $\text{As}_2\text{O}_3$ , arsenolite (cubic, *c*- $\text{As}_2\text{O}_3$ ), and claudetite (monoclinic, *m*- $\text{As}_2\text{O}_3$ ). The *g*- $\text{As}_2\text{O}_3$  sample was made by heating the crystalline arsenolite form of  $\text{As}_2\text{O}_3$  to 800 °C in a vacuum-sealed quartz tube (melting point  $\text{As}_2\text{O}_3=312.3$  °C). The glass was formed by letting the liquid cool in air, which is made by removing the sealed quartz tube from the furnace. The claudetite crystals were synthesized from crystalline arsenolite, which is sealed in a Pyrex tube with a trace amount of water and heated to 180 °C for 72 h. The claudetite sample was characterized by using both x-ray diffraction and Raman spectroscopy.

*In situ* high-pressure experiments were performed by using a cylindrical type diamond anvil cell (DAC).<sup>15</sup> The cell was fitted with 200  $\mu\text{m}$  culet diamonds for the spectroscopy experiments and 300  $\mu\text{m}$  culets for the x-ray diffraction experiments. In all of the cases, the sample (piece of glass, piece of claudetite crystal, or crystalline powder of arsenolite) was packed along with a few pieces of ruby smaller than 1  $\mu\text{m}$  in a 90  $\mu\text{m}$  diameter hole electroeroded in a rhenium gasket by using an electric discharge machine (Hylozoic Products) without a pressure transmitting medium. The pressure was determined by using the ruby fluorescence technique<sup>16</sup> in all of our high-pressure experiments that used a diamond anvil cell.

The Raman spectroscopy experiments were performed by using a custom-built notch filter based micro-Raman system that used a frequency-doubled yttrium aluminum garnet Verdi laser (Coherent, Inc.), which generates a narrow frequency single line at 532 nm. The laser excitation was focused onto the diamond anvil cell by using a 20 $\times$  long working distance Mitutoyo objective. The laser power after the objective was maintained between 5 and 7 mW to prevent damaging the sample. The signal was collected into a Shamrock 303i spectrometer (Andor Technology, Inc.) after removing the laser light by using two Kaiser supernotch filters. The signal was then diffracted off a 1200 grooves/mm grat-

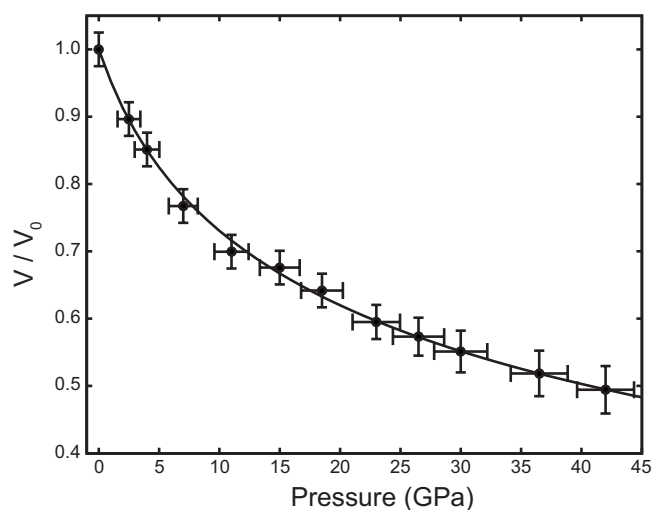


FIG. 2. Equation of state for  $\text{As}_2\text{O}_3$  glass. The solid line overlaid on the data is the Birch–Murnaghan equation of state fit of the data ( $B_0=18\pm 2$  GPa and  $B'_0=3.5\pm 0.5$  GPa).

ing and collected into a back-thinned Andor DV401-BR-DD charge coupled device detector. The spectral resolution of the system was 2  $\text{cm}^{-1}$ , which was high enough for the study of glasses and amorphous materials.

The x-ray diffraction experiment on *g*- $\text{As}_2\text{O}_3$  was performed on sector 1 at the Advanced Photon Source (Argonne National Laboratory, IL) by using a  $50\times 50$   $\mu\text{m}^2$  focused beam at a wavelength of 0.1241 Å (100 keV). The diamond anvil cell was fitted with one perforated diamond anvil on the upstream side of the cell to reduce the Compton scattering from diamond. The typical sample to detector distance was about 245 mm. The detector was a highly sensitive, low background GE Revolution amorphous Si area detector. The data were calibrated by using the diffraction pattern from  $\text{CeO}_2$ . The two-dimensional data were radially integrated by using the program<sup>17</sup> FIT2D and manually processed by using the method described in a previous paper.<sup>18</sup> Due to experimental time constraints, we selected four pressures at which to collect the diffraction data: 4, 17, 22, and 32 GPa. To properly normalize the radial distribution functions and extract coordination numbers, we carefully measured the equation of state of  $\text{As}_2\text{O}_3$  glass, which is presented in Fig. 2. We directly measured the equation of state by measuring the volume of a sample of  $\text{As}_2\text{O}_3$  glass packed in the gasket hole of the diamond anvil cell. The area of the cylindrical sample was measured by using digital images of the sample at each pressure point. The thickness of the sample was determined by measuring the distance between the two opposite diamond tables (face of the diamond parallel to the culet facing the outside of the cell) while taking into account the change in the diamond heights with pressure. The change in the diamond anvil heights with pressure was calibrated by using the known equation of state of KBr and CsCl.<sup>19</sup> We confirm the initial slope of the equation of state up to 7 GPa by measuring the equation of state in a pentane-isopentane hydrostatic medium. A fit of the  $\text{As}_2\text{O}_3$  data collected up to 42 GPa to a Birch–Murnaghan equation of state gave  $B_0=18\pm 2$  GPa and  $B'_0=3.5\pm 0.5$  GPa (Fig. 2).

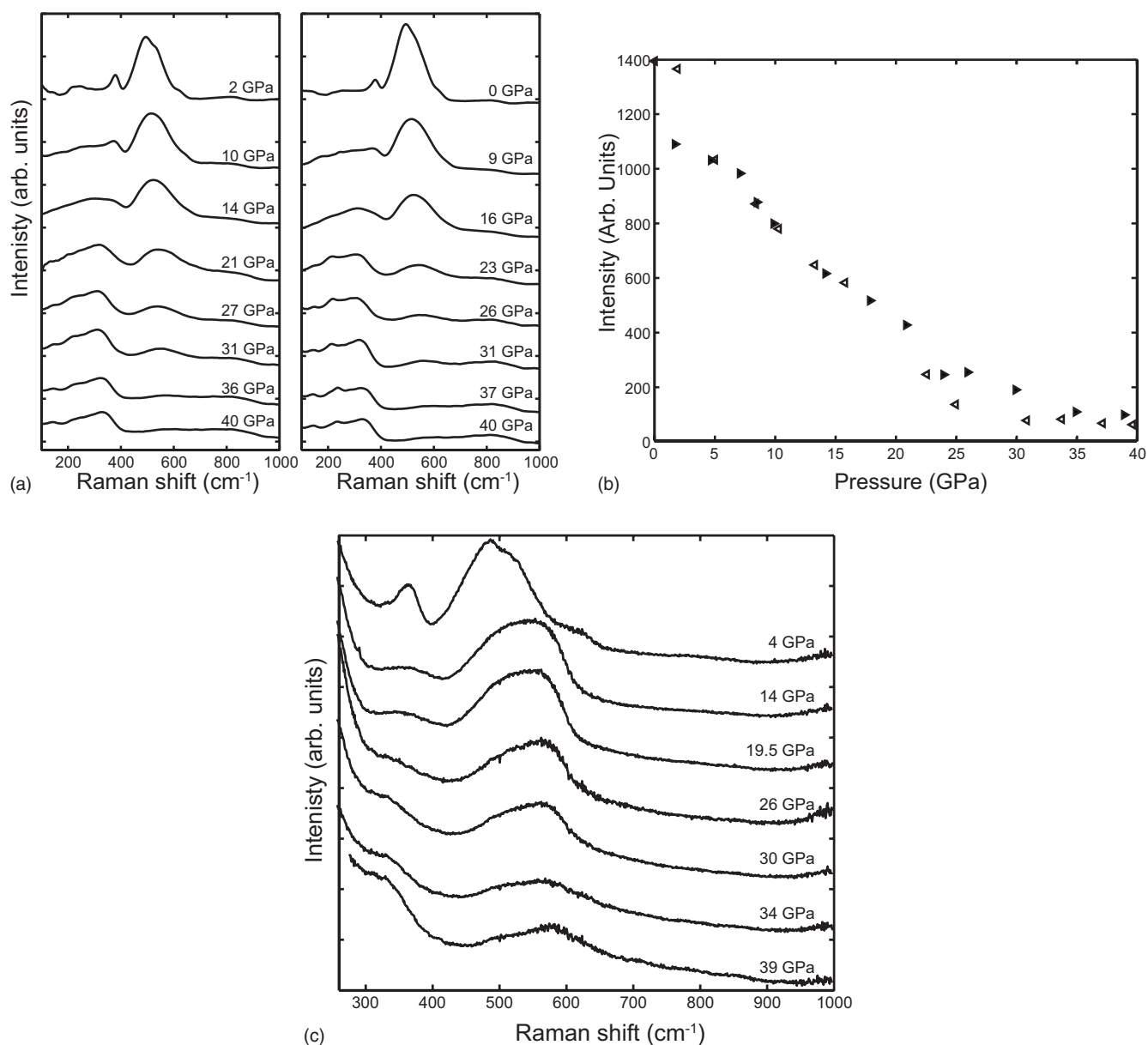


FIG. 3. (a) Raman spectra of  $\text{As}_2\text{O}_3$  glass ( $g\text{-As}_2\text{O}_3$ ) from ambient up to 40 GPa during compression (left) and decompression (right). The intensity of each spectrum collected at pressures  $>22$  GPa was multiplied by 2. (b) Integrated intensity from 400 to 800  $\text{cm}^{-1}$  as a function of pressure for  $g\text{-As}_2\text{O}_3$ . The solid triangles pointing to the right indicate data collected upon compression and the empty triangles pointing to the left indicate data collected upon decompression. (c) Raman spectra of  $\text{As}_2\text{O}_3$  glass from ambient to 39 GPa measured by using a 785 nm laser excitation wavelength.

### III. EXPERIMENTAL RESULTS

#### A. Raman spectroscopic study

##### 1. Compression-decompression of $g\text{-As}_2\text{O}_3$

The Raman spectrum of  $\text{As}_2\text{O}_3$  glass is composed of a very intense broad feature centered about 500  $\text{cm}^{-1}$  preceded by a less intense and sharper feature centered at 380  $\text{cm}^{-1}$ . According to Andrikopoulos *et al.*,<sup>13</sup> the large feature can be separated into four components (480, 525, 550, and 610  $\text{cm}^{-1}$ ). The 380 and 525  $\text{cm}^{-1}$  peaks are characteristic of cage-like regions of the glass, and the 480 and 550  $\text{cm}^{-1}$  peaks are assigned to layer-like configurations.<sup>13,20</sup>

We measured the *in situ* the Raman spectrum of  $\text{As}_2\text{O}_3$  glass in the diamond anvil cell up to 40 GPa (Fig. 3). Upon compression, the Raman scattering intensity progressively decreases. The main feature in the glass spectrum also seems to become less resolved, and at 15 GPa, the four peaks are not discernable and only a broad feature centered around 500  $\text{cm}^{-1}$  can be observed. Above 20 GPa, a different feature appears below 400  $\text{cm}^{-1}$ , while the large peak between 400 and 600  $\text{cm}^{-1}$  dramatically weakens. Beyond 30 GPa, the 500  $\text{cm}^{-1}$  feature has completely disappeared and only the low frequency feature is present on the pattern. Upon decompression, the dramatic change in the Raman spectrum appears to be reversible and the large feature between 400

and  $600\text{ cm}^{-1}$  regains intensity below 25 GPa. After a complete decompression of the sample, the Raman spectra are almost identical. The reversibility of the changes in the Raman spectra shows little or no hysteresis [Fig. 3(b)], which is possibly due to the rigid nature of the  $\text{AsO}_3$  pyramids.

It should also be noticed that upon compression, the sample changes color from completely clear to yellow, then red, and, finally, completely black above 45 GPa. This phenomenon is also observed in similar glasses such as  $\text{As}_2\text{S}_3$ .<sup>21</sup> Since the absorption of the sample at 532 nm significantly increases above 30 GPa, we also reproduced the experiment by using a lower energy laser wavelength of 785 nm and observed the same transition [Fig. 3(c)]. This was done to ensure that no photoinduced effects were being caused by the Raman excitation laser.

## 2. Compression-decompression of arsenolite

Arsenolite has 20 internal vibrational modes, of which 10 are Raman active (two  $A_{1g}$ , two  $E_g$ , and four  $F_{2g}$ ) and 4 are IR active ( $F_{1u}$ ). The Raman spectrum of arsenolite shows seven strong vibrations between 100 and  $1000\text{ cm}^{-1}$  (Fig. 4). The peak at  $559$  and  $368\text{ cm}^{-1}$  are assigned to out of phase and in phase breathing of As and O in the  $\text{As}_4\text{O}_6$  molecule, respectively.<sup>12</sup> The peaks at  $182$  and  $413\text{ cm}^{-1}$  are assigned to the bending of As-O-As. The peaks at  $780$  and  $470\text{ cm}^{-1}$  are due to As-O-As stretching. Finally, the peak at  $266\text{ cm}^{-1}$  is an As-O-As wagging mode.<sup>22</sup>

Upon compression to 15 GPa, the Raman spectrum shows changes in relative intensities as previously reported by Grzechnik.<sup>12</sup> Along with the changes, the Raman scattering intensity of the peaks have become much weaker and some broad features start to appear underneath the spectrum. The spectra collected at higher pressures ( $P > 25$  GPa) show a dramatic decrease in remaining intensity of the arsenolite vibrations. The pattern starts to look more and more like that of  $g\text{-As}_2\text{O}_3$  at the same pressures. The strong  $370\text{ cm}^{-1}$  arsenolite peak due to the breathing of  $\text{As}_4\text{O}_6$  units drastically reduces in intensity. Above 30 GPa, the patterns do not show any sharp band, and only a large broad feature is visible below  $400\text{ cm}^{-1}$ . To confirm that the sample is, indeed, amorphizing, we also performed the same experiment by using x-ray diffraction [Fig. 4(b)] and observed that the sample does lose long-range order and become amorphous with respect to x-ray diffraction as well.

Upon decompression, the pattern remains unchanged down to 28 GPa. At 25 GPa, one weak arsenolite peak appears at  $346\text{ cm}^{-1}$  on top of the broad background and a different broad feature appears between 400 and  $600\text{ cm}^{-1}$ . Upon further decompression, the intensity of the low wave number broad feature decreases and completely disappears below 15 GPa. The intensity of the feature centered at  $500\text{ cm}^{-1}$  increases and a few more arsenolite peaks become visible. When the experiment is repeated by using a 785 nm laser excitation line, the exact same result is observed.

## 3. Compression of claudetite

The Raman spectrum of claudetite was previously described by Mercier and Sourisseau.<sup>23</sup> A factor group analysis

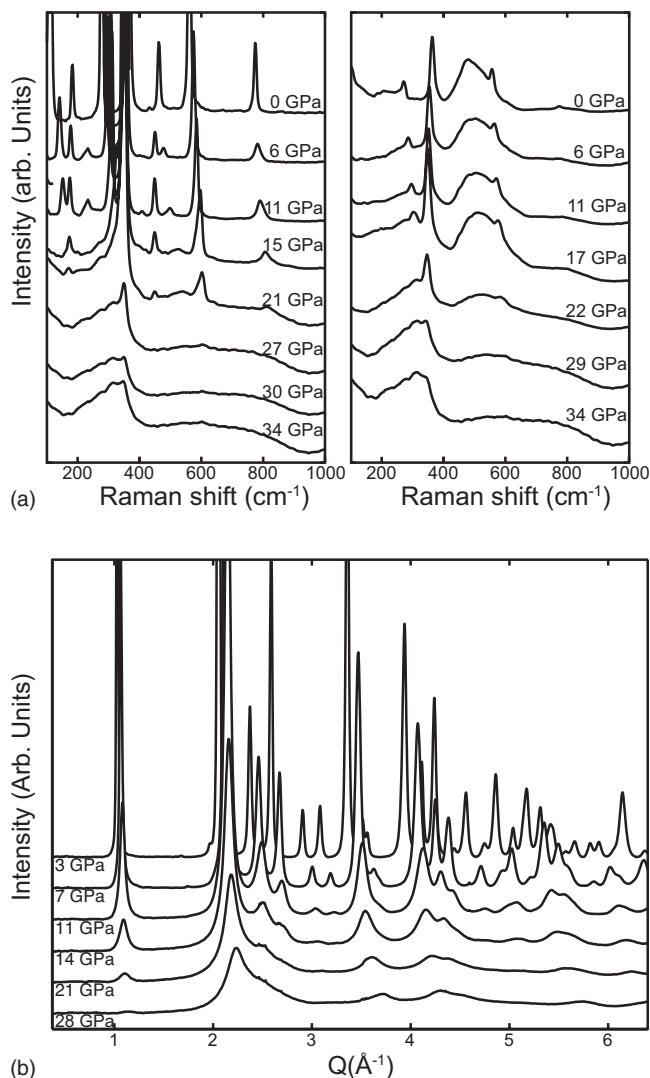


FIG. 4. (a) Raman spectra of arsenolite  $c\text{-As}_2\text{O}_3$  from ambient up to 34 GPa during compression (left) and decompression (right). (b) X-ray diffraction patterns for arsenolite as a function of increasing pressure.

of the claudetite structure shows that there are 54 internal modes, of which 14  $B_g$  and 13  $A_g$  modes are Raman active and 14  $B_u$  and 13  $A_u$  modes are infrared active. The Raman spectrum of claudetite at 2.5 GPa displays nine major peaks below  $400\text{ cm}^{-1}$ , one very strong peak at  $474.5\text{ cm}^{-1}$  (breathing mode of O normal to the layers), followed by three less intense peaks at 559 (symmetric stretching of the  $\text{AsO}_3$  pyramids), 638.5, and  $652.5\text{ cm}^{-1}$  (asymmetric stretching of the  $\text{AsO}_3$  pyramids) and, finally, three weaker peaks between 700 and  $900\text{ cm}^{-1}$  (asymmetric stretching of the  $\text{AsO}_3$  pyramids) (Fig. 5). Upon compression, the main features of the spectrum remain unchanged and some additional peaks seem to appear. Two intense peaks appear on either side of the main band and the relative intensity of the weak peaks below  $400\text{ cm}^{-1}$  (symmetric deformation of the  $\text{AsO}_3$  pyramids) increases as compared to that of the strongest peak. Up to 40 GPa, the sample remained clearly crystalline in character and the main peak retains the same full width at half maximum. The apparent broadening above 30

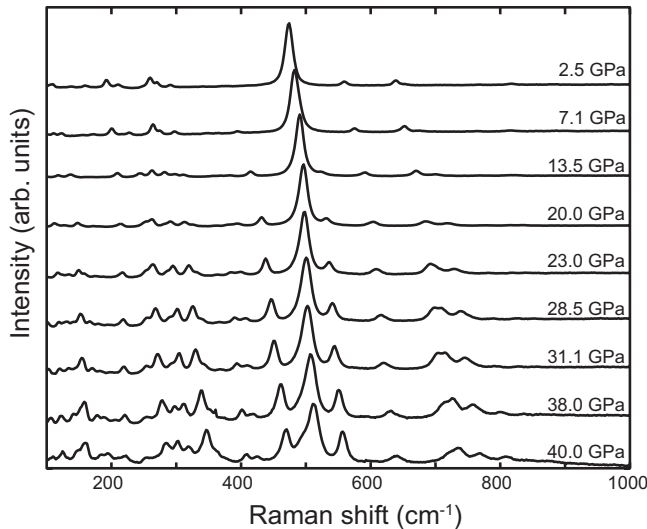


FIG. 5. High-pressure Raman spectra of claudetite ( $m\text{-As}_2\text{O}_3$ ) from ambient up to 40 GPa.

GPa is due only to the splitting of the peak. At 40 GPa, we can clearly observe a shoulder developing on the high energy side of that peak. No pressure-induced amorphization was observed within our experimental pressure range for the claudetite polymorph. Only minor changes occur, which result in the appearance of some other Raman active vibrations and some changes in relative intensity.

#### 4. Diamond anvil cell Raman spectroscopy summary

The Raman study of  $\text{As}_2\text{O}_3$  showed that an amorphous-amorphous transition<sup>24</sup> occurs upon compression of  $g\text{-As}_2\text{O}_3$  above 20 GPa (Fig. 3). This transition is characterized by a rapid decrease in intensity of the  $550\text{ cm}^{-1}$  mode and a corresponding appearance of an additional low frequency mode at  $350\text{ cm}^{-1}$ , which begins to appear above 20 GPa. That transition is reversible upon decompression with little or no hysteresis [Fig. 3(b)]. The compression of arsenolite also yielded pressure-induced amorphization (Fig. 4). The arsenolite pattern progressively gives way to an amorphous pattern between 16 and 27 GPa. At 27 GPa, the pattern is very similar to that obtained for glassy  $\text{As}_2\text{O}_3$  at the same pressure. Finally, we also compressed claudetite and observe no pressure-induced amorphization. Andrikopoulos *et al.*<sup>13</sup> previously described the changes in the glass spectrum below 10 GPa to be due to a reduction in the intensity of modes characteristic of the cagelike configuration with respect to the modes assigned to the layerlike regions. This observation would, in fact, not be consistent with the subsequent disappearance of the Raman intensity in the  $400\text{--}600\text{ cm}^{-1}$  region since claudetite, which is the layered structure form of  $\text{As}_2\text{O}_3$ , is kinetically stable at ambient temperature up to at least 40 GPa. Both arsenolite and  $\text{As}_2\text{O}_3$  glass transform into the same structure above the same transition pressure. Therefore, the Raman studies presented here would suggest that the low-pressure glass structure (glass synthesized at room pressure) is more closely related to the arsenolite structure, which is in agreement with the neutron diffraction results of Clare *et al.*<sup>7</sup>

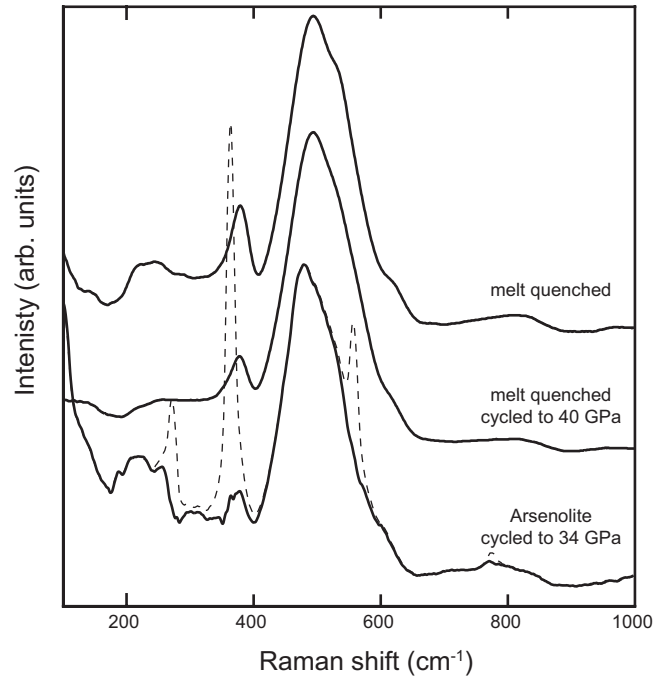


FIG. 6. Comparison of thermally quenched  $g\text{-As}_2\text{O}_3$  before and after pressurization to 40 GPa along with pressure amorphized  $c\text{-As}_2\text{O}_3$  (arsenolite) at room pressure (dashed line). We also plotted with a solid line the pressure amorphized pattern after the subtraction of the arsenolite peaks (dashed line) to better visualize the Raman spectrum of the amorphous material.

In Fig. 6, we can see that there is a little or no difference between the Raman spectra of  $g\text{-As}_2\text{O}_3$  and pressure cycled (to 40 GPa)  $g\text{-As}_2\text{O}_3$ . Along with the two patterns of  $g\text{-As}_2\text{O}_3$ , we plotted the pattern of pressure amorphized arsenolite. To clarify Fig. 6, we subtracted the arsenolite spectrum from the pressure amorphized pattern. We see in Fig. 6 that the pressure amorphized spectrum shows no significant difference from the  $g\text{-As}_2\text{O}_3$  pattern. This observation indicates a very similar structure for the pressure amorphized arsenolite, the pressure cycled  $\text{As}_2\text{O}_3$  glass, and the thermally quenched  $\text{As}_2\text{O}_3$  glass. Mei *et al.*<sup>14</sup> reported an *ex situ* structural investigation of  $\text{As}_2\text{O}_3$  glass recovered from 10 and 23 GPa. They concluded that the structure of the recovered glass is very similar to that of the starting glass material with only a small amount of residual densification. This result is consistent with our results from samples recovered from 40 GPa.

#### B. X-ray diffraction study of $g\text{-As}_2\text{O}_3$

To better understand the local structural changes occurring across the transition observed in our Raman spectroscopy study, we performed an *in situ* DAC x-ray diffraction experiment. We collected data upon compression from 4 up to 32 GPa and on the pressure quenched sample.

The total structure factor at each pressure is presented in Fig. 7. The ambient pattern was previously collected outside the DAC by Mei *et al.*<sup>14</sup> The sharp weak peaks sitting on top of the broad amorphous diffraction pattern at high pressure

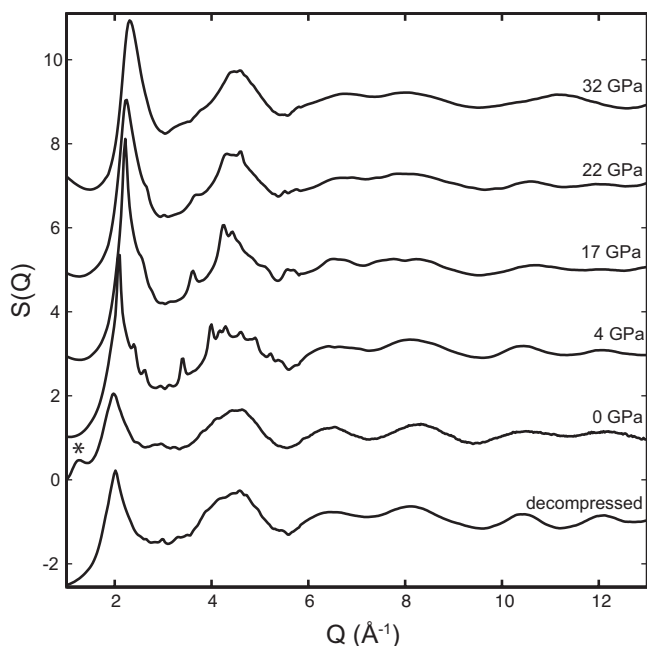


FIG. 7. Total structure factor  $S(Q)$  before compression at ambient outside the diamond anvil cell (RP) and as a function of pressure *in situ* in the diamond anvil, and, finally, after decompression still in the diamond anvil cell. The high-pressure data are successively vertically shifted up by 2 units and the decompressed plot is shifted down by 2 units. The \* on the room pressure data indicates the first sharp diffraction peak. The peak is not observed in any of the other patterns. The sharp peaks in the diffraction patterns at 4 and 17 GPa are due to a small amount (<1%) of arsenolite present in the sample.

are due to a small amount of crystalline arsenolite present in the glass. Arsenolite recrystallizes readily from the glass when a trace amount of moisture is present. The relative intensity of the peaks as compared to the broad features characteristic of the glass indicates that only a very small fraction (a few percent) of the sample is crystalline. The total structure factor of  $g\text{-As}_2\text{O}_3$  shows a very weak first sharp diffraction peak, which disappears completely upon initial compression. This change would indicate a loss of medium range order upon compression of  $\text{As}_2\text{O}_3$  glass, which is associated with the shrinkage of open regions in the network. Up to 17 GPa, the short-range order of the glass ( $Q > 5 \text{ \AA}^{-1}$ ) shows a general broadening of the oscillations. From 17 up to 32 GPa, some changes become noticeable as the oscillations are clearly different from that observed at ambient conditions. These changes indicate significant structural modifications in the short-range order of  $g\text{-As}_2\text{O}_3$  at the highest pressures. The principal peak shifts from  $1.97$  to  $2.31 \text{ \AA}^{-1}$  with an increase in height of almost 60%, which is associated with an increase in the amount of extended range order with pressure.<sup>25</sup>

The first peak in the pair distribution function shown in Fig. 8 results from the As-O bonds. The maximum in the distribution of As-O bond distance change from  $1.79 \pm 0.01 \text{ \AA}$  to  $1.82 \pm 0.01 \text{ \AA}$  between 0 and 32 GPa and returns to  $1.79 \pm 0.01 \text{ \AA}$  in the decompressed glass. The bond distances can be compared to the ambient As-O dis-

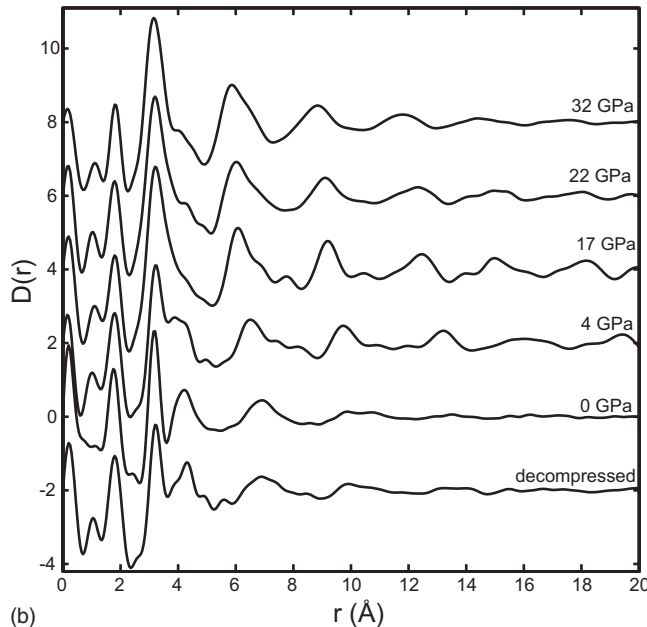
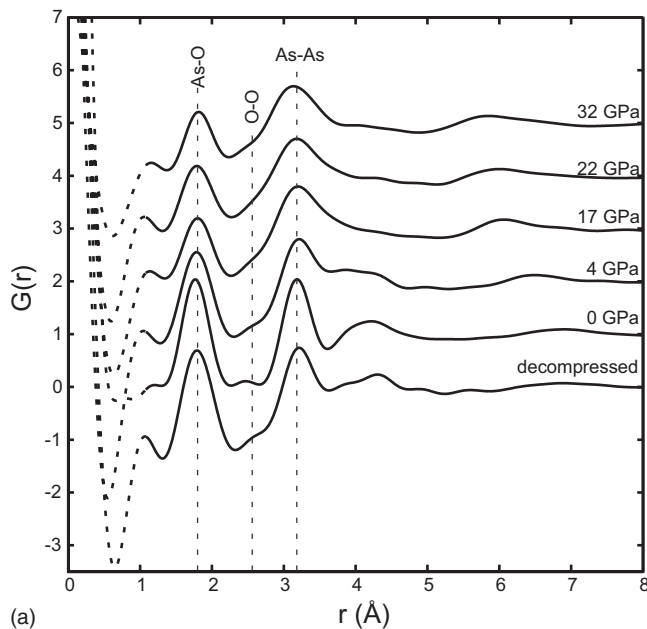


FIG. 8. (a) Total pair distribution function  $G(r)$  and (b) differential distribution function  $D(r) = 4\pi\rho[G(r) - 1]$  data for  $g\text{-As}_2\text{O}_3$  before compression at ambient and as a function of pressure *in situ* in the diamond anvil cell at 4, 17, 22, and 32 GPa and after decompression still in the diamond anvil cell. The high-pressure data are successively vertically shifted up by 1 unit and the decompressed plot is shifted down by 1 unit.

tances of  $c\text{-As}_2\text{O}_3$  and  $m\text{-As}_2\text{O}_3$  polymorphs, which are  $1.79$  and  $1.72\text{--}1.81 \text{ \AA}$ , respectively. At ambient, the second peak arises from As-As correlations. The position of the peak slightly changes with pressure from  $3.19 \pm 0.01 \text{ \AA}$  down to  $3.14 \pm 0.01 \text{ \AA}$  at 32 GPa. These changes in the As-As and As-O distances indicate a decrease in the As-O-As angle from  $126.0 \pm 1.0^\circ$  at ambient to  $120.0 \pm 1.0^\circ$  at 32 GPa if we assume that the bond angle distribution is symmetric. Along with the shortening of the correlation distance, the distribu-

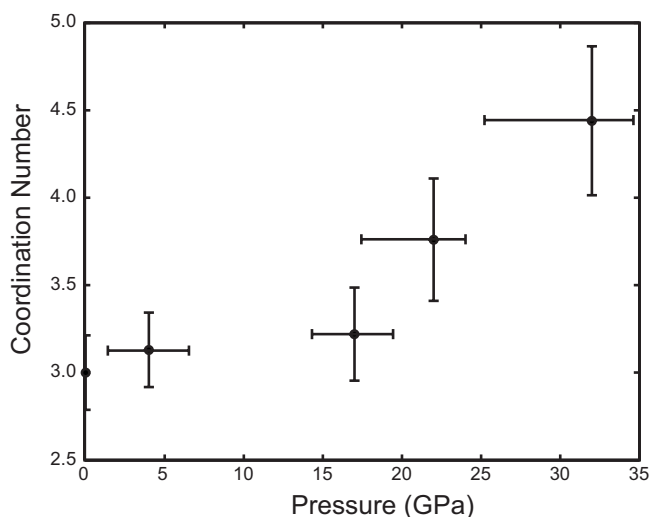


FIG. 9. Coordination number determined from the  $G(r)$  data for  $g\text{-As}_2\text{O}_3$  as a function of pressure.

tion noticeably broadens above 4 GPa. The broad peak centered at about 4 Å at ambient pressure merges with the 3.2 Å peak with increasing pressure, which indicates a less discrete distribution of As-As correlation distances. Upon pressure release, the total pair distribution function sharpens back up and the feature centered at 4 Å is once again resolved from the sharp 3.2 Å peak. Mei *et al.*<sup>14</sup> previously reported this observation for  $g\text{-As}_2\text{O}_3$  samples quenched from 10 and 23 GPa.

The analysis of the total pair distribution function also provides the number of oxygen atoms in the first coordination shell of arsenic. We know from previous studies that arsenic is coordinated to three oxygens ( $\text{AsO}_3$  units) at room pressure.<sup>6,7</sup> The integration under the As-O peak of  $G(r)r^2$  assuming form factors independent of  $Q$  for the room pressure data gives a coordination number of  $3.1 \pm 0.2$ , which is very close to the previously reported value.<sup>7</sup> At 32 GPa, we obtain a coordination number of  $4.6 \pm 0.4$ . Therefore, there is a clear increase in the first coordination shell of As (Fig. 9). The plot indicates that only a very little change in the coordination number is observed up to 17 GPa. However, between 17 and 22 GPa, the coordination increased from 3.2 to almost 3.8.

Upon pressure release, the As coordination comes back to the initial configuration, wherein arsenic is surrounded by three oxygen in the first coordination shell.

#### IV. DISCUSSION

Our experimental data on  $\text{As}_2\text{O}_3$  indicate that some structural changes occur in  $\text{As}_2\text{O}_3$  glass between 17 and 30 GPa. The x-ray diffraction data indicate an increase in the coordination number of oxygen atoms around As above 17 GPa. The average coordination number goes from  $3.0 \pm 0.2$  below 17 GPa to  $4.6 \pm 0.4$  at 32 GPa.

The As-O bond length very slightly elongates with pressure and its distribution remains sharp. In  $\text{As}_2\text{O}_5$ , arsenic is in four- and sixfold coordinations with O [Fig. 1(c)]. How-

ever, the bond distance for each As-O environment is very different. The  $^{\text{IV}}\text{As-O}$  bonds are 1.66–1.71 Å, while the  $^{\text{VI}}\text{As-O}$  bonds are 1.78–1.82 Å. Our x-ray data clearly show that the As-O bond distance only increases and shows no indication of any short As-O bond corresponding to  $\text{AsO}_4$  tetrahedra. This observation is consistent with a model wherein the As-O coordination changes from 3 to 6. The present analysis of the diffraction data does not show any obvious indication of four- or five-coordinated environments upon compression. The data do not show any plateau in the coordination number at 4, unlike in the case of  $\text{GeO}_2$ ,<sup>26</sup> wherein the coordination plateaus at 5, or  $\text{B}_2\text{O}_3$ ,<sup>27</sup> wherein the coordination plateaus at 4. This also indicates the absence of four-coordinated As.

The interpretation of the Raman data does not provide a direct indication of the coordination of As since the main peak position that is characteristic of octahedral  $\text{AsO}_6$  in  $\text{As}_2\text{O}_5$  is the peak at  $568 \text{ cm}^{-1}$  at ambient conditions.<sup>28</sup> This is comparable to the main peak in  $c\text{-As}_2\text{O}_3$ , which sits at about  $560 \text{ cm}^{-1}$ . In the  $\text{As}_2\text{O}_5$  structure, the Raman peaks characteristic of  $\text{AsO}_4$  tetrahedra are all fairly weak and lie mostly between 800 and  $950 \text{ cm}^{-1}$ .<sup>28</sup> From the analysis of the Raman intensity between 400 and  $600 \text{ cm}^{-1}$ , we very clearly see that there is no significant sign of any hysteresis in the transition, which is surprising since there is a large change in the structure of the glass with a change in coordination. We also observed that whether we start from an arsenolite crystalline sample (lowest potential energy phase) or a glass sample (higher potential energy phase), the transition occurs at the same pressure and the high density amorphous phase has the same structure according to Raman spectroscopy. Upon decompression, the sample recovered at room pressure from amorphization of arsenolite or pressure cycling of  $\text{As}_2\text{O}_3$  glass is nearly identical to the  $\text{As}_2\text{O}_3$  glass melt quenched at room pressure (Fig. 6 and 7). The only significant difference is in the Raman intensity of the peak at  $377 \text{ cm}^{-1}$ , which corresponds to cagelike  $\text{As}_4\text{O}_6$  units.<sup>20</sup>

The transition in  $\text{As}_2\text{O}_3$  can be compared to that in  $\text{Bi}_2\text{O}_3$  and  $\text{B}_2\text{O}_3$ , both of which display a change in coordination upon compression.<sup>29,27</sup>  $\text{Bi}_2\text{O}_3$  pressure amorphizes just like arsenolite and is recovered into an amorphous phase at ambient pressure.<sup>29</sup> The authors also reported a strong coloration of the  $\text{Bi}_2\text{O}_3$  sample with pressure just like what we observed for  $\text{As}_2\text{O}_3$  glass and arsenolite. The  $\text{Bi}_2\text{O}_3$  sample changed from pale yellow at room pressure to bright red at 24 GPa. The study on  $\text{B}_2\text{O}_3$  shows that the coordination shell changes progressively from three to four oxygen atoms surrounding each B upon compression.<sup>27</sup> The change is continuous and the data showed that the ratio of  $\text{BO}_3$  to  $\text{BO}_4$  changes with pressure.

#### V. CONCLUSION

In conclusion, we studied  $\text{As}_2\text{O}_3$  up to 40 GPa. Above 20 GPa, we see the onset of a structural transformation that results in a complete loss of the Raman intensity above  $400 \text{ cm}^{-1}$  in  $g\text{-As}_2\text{O}_3$  and  $c\text{-As}_2\text{O}_3$  (arsenolite).  $c\text{-As}_2\text{O}_3$  amorphizes above 20 GPa into a phase with a structure very consistent with that of  $g\text{-As}_2\text{O}_3$  at the same pressure. The

Raman spectrum of the low-pressure glass is recovered upon decompression in both *c*-As<sub>2</sub>O<sub>3</sub> and *g*-As<sub>2</sub>O<sub>3</sub>. The compression of *m*-As<sub>2</sub>O<sub>3</sub> (claudetite) displayed no sign of amorphization. This observation is consistent with the previous reports, which suggested that the structure of *g*-As<sub>2</sub>O<sub>3</sub> is much more closely related to that of *c*-As<sub>2</sub>O<sub>3</sub> than that of *m*-As<sub>2</sub>O<sub>3</sub>.<sup>6,7</sup>

Based on the x-ray diffraction data collected on *g*-As<sub>2</sub>O<sub>3</sub> as a function of pressure, it was concluded that an increase in the average As coordination number from three oxygen atoms to almost five at 32 GPa occurred. The increase in coordination appears to start only above 17 GPa. Based on the known crystalline As-O bond lengths, the transition is interpreted as a progressive change in the ratio of three-coordinated and six-coordinated As-O polyhedra without the formation of four-coordinated As. This transition is com-

parable to that of B<sub>2</sub>O<sub>3</sub>, which progressively changes from threefold to fourfold coordination. The amorphous-amorphous transition in As<sub>2</sub>O<sub>3</sub> shows no hysteresis.

#### ACKNOWLEDGMENTS

R. T. Hart is thanked for his help during the initial stages of the study. The use of the Advanced Photon Source was supported by the U.S. Department of Energy, Basic Energy Sciences, Office of Science, under Contract No. W-31-109-Eng-38. This work was supported by the National Science Foundation (Chemistry Division, Grant No. 0612553), U.S. Department of Energy, and Carnegie/DOE Alliance Center (DOE-NNSA) CDAC.

\*Corresponding authors.

†esoignar@usa.net

‡jyarger@gmail.com

<sup>1</sup>F. Pertlik, Czech. J. Phys., Sect. B **B28** (2), 170 (1978).

<sup>2</sup>F. Pertlik, Monatsch. Chem. **109**, 277 (1978).

<sup>3</sup>F. Pertlik, Monatsch. Chem. **106**, 755 (1975).

<sup>4</sup>W. B. White, F. Datchell, and R. Roy, Z. Kristallogr. **125**, 450 (1967).

<sup>5</sup>E. Kordes, Z. Phys. Chem. Abt. B **B43**, 173 (1939).

<sup>6</sup>M. Imaoka and H. Hasegawa, Phys. Chem. Glasses **21**, 67 (1980).

<sup>7</sup>A. G. Clare, A. C. Wright, R. N. Sinclair, F. I. Galeener, and A. E. Geissberger, J. Non-Cryst. Solids **111**, 123 (1989).

<sup>8</sup>G. N. Papatheodorou and S. A. Solin, Phys. Rev. B **13**, 1741 (1976).

<sup>9</sup>F. L. Galeener, G. Lucovsky, and R. H. Geils, Phys. Rev. B **19**, 4251 (1979).

<sup>10</sup>S. N. Yannopoulos, G. N. Papatheodorou, and G. Fytas, Phys. Rev. B **60**, 15131 (1999).

<sup>11</sup>R. Bohmer, K. Ngai, C. Angell, and D. Plazek, J. Chem. Phys. **99**, 4201 (1993).

<sup>12</sup>A. Grzechnik, J. Solid State Chem. **144**, 416 (1999).

<sup>13</sup>K. S. Andrikopoulos, D. Christofilos, G. A. Kourouklis, and S. N. Yannopoulos, High Press. Res. **26**, 401 (2006).

<sup>14</sup>Q. Mei, R. T. Hart, C. J. Benmore, S. Amin, K. Leinenweber, and J. L. Yarger, J. Non-Cryst. Solids **353**, 1755 (2007).

<sup>15</sup>E. Soignard and P. F. McMillan, in *High-Pressure Crystallography*, edited by A. Katrusiak and P. F. McMillan (Kluwer, Dordrecht, 2004), Vol. 140, p. 81.

<sup>16</sup>H. K. Mao, J. Xu, and P. M. Bell, J. Geophys. Res. **91**, 4673

(1986).

<sup>17</sup>A. P. Hammersley, S. O. Svensson, M. Hanfland, A. N. Fitch, and D. Häusermann, High Press. Res. **14**, 235 (1996).

<sup>18</sup>Q. Mei, C. J. Benmore, E. Soignard, S. Amin, and J. L. Yarger, J. Phys.: Condens. Matter **19**, 415103 (2007).

<sup>19</sup>U. Kohler, P. G. Johannser, and W. B. Holzapfel, J. Phys.: Condens. Matter **9**, 5581 (1997).

<sup>20</sup>G. Lucovsky and F. Galeener, J. Non-Cryst. Solids **37**, 53 (1980).

<sup>21</sup>J. M. Besson, J. Cernogora, M. L. Slade, B. A. Weinstein, and R. Zallen, Physica B (Amsterdam) **105**, 319 (1981).

<sup>22</sup>J. O. Jensen, S. J. Gilliam, A. Banerjee, D. Zeroka, S. J. Kirkby, and C. N. Merrow, J. Mol. Struct. **664-665**, 145 (2003).

<sup>23</sup>R. Mercier and C. Sourisseau, Spectrochim. Acta, Part A **34**, 337 (1978).

<sup>24</sup>V. V. Brazhkin, A. G. Lyapin, O. V. Stalgorova, E. L. Gromnitskaya, S. V. Popova, and O. B. Tsiok, J. Non-Cryst. Solids **212**, 49 (1997).

<sup>25</sup>P. S. Salmon, R. A. Martin, P. E. Mason, and G. J. Cuello, Nature (London) **435**, 75 (2005).

<sup>26</sup>M. Guthrie, C. A. Tulk, C. J. Benmore, J. Xu, J. L. Yarger, D. D. Klug, J. S. Tse, H.-k. Mao, and R. J. Hemley, Phys. Rev. Lett. **93**, 115502 (2004).

<sup>27</sup>S. K. Lee, P. J. Eng, H.-K. Mao, Y. Meng, M. Newville, M. Y. Hu, and J. Shu, Nat. Mater. **4**, 851 (2005).

<sup>28</sup>H. Ehrhardt, and M. Jansen, Z. Anorg. Allg. Chem. **504**, 128 (1983).

<sup>29</sup>C. Chouinard and S. Desgreniers, Solid State Commun. **113**, 125 (1999).